# STRATEGIES

# FOR FUTURE CLIMATE RESEARCH

# STRATEGIES FOR FUTURE CLIMATE RESEARCH*)

Edited by Mojib Latif

*)A collection of papers presented at the birthday colloquium in honour of Klaus Hasselmann's 60th anniversary.

Max-Planck-Institut für Meteorologie
Bundesstraße 55
D-2000 Hamburg 13

# POP Art

Hans von Storch, Gerd Bürger, Reiner Schnur and Jinsong Xu

**Abstract**

Principal Oscillation Patterns (POPs) may be seen as normal modes of a linearized system whose system matrix is estimated from data. To demonstrate this viewpoint we show that the best defined POPs of tropospheric day-to-day variability coincide with the most unstable modes derived from linearized theory.

The conventional POP analysis technique has been generalized in two ways. In the *cyclostationary* POP analysis, the estimated system matrix is allowed to vary deterministically with the annual cycle. In the *complex* POP analysis not only the state of the system but also its "momentum" is modeled.

## 1. Introduction

The *POP* (*Principal Oscillation Pattern*) analysis is a multivariate technique to empirically infer the characteristics of the space-time variations of a complex dynamical system (Hasselmann, 1988; von Storch et al., 1988, 1990; Penland, 1989). The basic approach is to consider the system as first-order auto-regressive process which is fitted to the data. An alternative way to regard POPs is as a vulgarized[1] version of Principal Interaction Patterns (PIPs) where the dynamics of a system with possibly many degrees of freedom are approximated by a (linear or nonlinear) model with only a few free parameters (Hasselmann, 1988; Storch et al., 1990). Then, the space-time characteristics of the low-order system are regarded as being the same as those of the full system.

In the present paper we review the state of the art of POP analysis including two recent off-springs, the *cyclostationary* (Alonso et al. (1991) and Blumenthal (1990)) and the *complex* POP analysis (Bürger, 1991).

Nowadays the POP analysis is a routinely used tool (Gallagher et al., 1991) to study space-time statistics in the climate system. Processes analysed with POPs are the Madden and Julian Oscillation (MJO) (Storch et al., 1988; Storch and Xu, 1990; Storch and Baumhefner, 1991; Storch and Smallegange, 1991), oceanic variability (Latif[2] and Villwock, 1989; Xu, 1990; Mikolajewicz, 1990), the stratospheric Quasi-Biennial Oscillation (QBO) (Xu, 1991a), the Southern Oscillation (SO) (Xu and Storch, 1990; Xu, 1990), tropospheric baroclinic waves (Schnur et al., 1991) and low-frequency variability in the coupled atmosphere-ocean system (Xu, 1991b)

In Section 2 of this paper the POPs are introduced as normal modes of a linear system the parameters of which are inferred from a stationary vector time series.

---

[1]See Marx (1864, p. 912) on *vulgarization* and the name *von Storch*.

[2]Because of limited space we do not quote Latif and Flügel (1990) and Latif et al (1991).

In Section 3 two examples of a POP analysis are given. The example on the tro-pospheric baroclinic waves (Schnur et al., 1991) demonstrates the normal mode concept of the POPs. The best defined POPs coincide with the most unstable modes derived in a conventional stability analysis of the linearized dynamical equations. The other example is the joint POP analysis of tropospheric and stratospheric data (Xu, 1991a): two independent modes with similar time scales, the Southern Oscillation (SO) and the Quasi-Biennial Oscillation (QBO), are identified.

In Sections 4 and 5, two generalizations of the POP analysis are presented: the cyclostationary POP analysis and the complex POP analysis.

Since a POP analysis is based on the fit of a time series model to the data, the POP approach has a predictive potential (Xu and Storch, 19990; Storch and Xu, 1990). We will not consider this aspect in the present paper.

## 2. POPs, Normal Modes and Multivariate Spectral Analysis

The following notation is used: Vectors are given in **bold** and matrices are given in gothic. If $\mathfrak{A}$ is a matrix then $\mathfrak{A}^T$ is the transposed matrix. If x is any complex quantity then $x^*$ is its complex conjugate.

It should be noted that the POP formalism - conventional, cyclostationary and complex POP analysis - may be applied to linear systems whose system matrices are estimated from data or whose system matrices are derived from theoretical dynamical considerations (see also Section 3a).

The normal modes of a linear discretized real system

(1) $\mathbf{X}(t+1) = \mathfrak{A} \cdot \mathbf{X}(t)$

are the eigenvectors $\mathbf{P}$ of the matrix $\mathfrak{A}$. In general, $\mathfrak{A}$ is not symmetric and some or all of its eigenvalues $\lambda$ and eigenvectors $\mathbf{P}$ are complex. However, since $\mathfrak{A}$ is a real matrix the complex conjugate quantities $\lambda^*$ and $\mathbf{P}^*$ also satisfy the eigen-equation $\mathfrak{A} \cdot \mathbf{P}^* = \lambda^* \mathbf{P}^*$. In most cases, all eigenvalues are different and the eigenvectors form a linear basis. Then each state $\mathbf{X}$ may be uniquely expressed in terms of the eigenvectors,

(2) $\mathbf{X} = \sum_j z_j \cdot \mathbf{P}_j$ for j = 1,...n.

The coefficients of the pairs of complex conjugate eigenvectors are complex conjugate, too. Inserting (2) into (1) we find that the coupled system (1) becomes uncoupled, yielding n single equations:

(3) $z_j(t+1) = \lambda_j \cdot z_j(t)$ for j = 1,...n, or

(4) $z_j(t) = \lambda_j^t \cdot z_j(0)$.

The contribution $\mathbf{p}(t)$ of a complex conjugate pair $\mathbf{P},\mathbf{P}^*$ to the process $\mathbf{X}(t)$ is given by (the index is disregarded for convenience)

$$\mathbf{p}(t) = z(t) \cdot \mathbf{P} + [z(t) \cdot \mathbf{P}]^*$$

or

(5) $\mathbf{p}(t) = z^1(t) \cdot \mathbf{P}^1 - z^2(t) \cdot \mathbf{P}^2$

with $\mathbf{P} = \mathbf{P}^1 + i \cdot \mathbf{P}^2$ and $2z(t) = z^1(t) + i \cdot z^2(t)$.

Now it is easy to see how the modes of a linear system evolve. Using (4) and $\lambda = \rho \cdot exp(i\eta)$ equation (5) gets the new form:

(6) $\mathbf{p}(t) = \rho^t \cdot ( \cos(\eta t) \cdot \mathbf{P}^1 - \sin(\eta t) \cdot \mathbf{P}^2 )$ .

The simple geometric meaning of (6) is: the trajectory $\mathbf{p}(t)$ is a spiral in the two-dimensional $\mathbf{P}^1/\mathbf{P}^2$-phase space with period $T = 2\pi/\eta$ and e-folding time $\tau = -1/\ln(\rho)$. The system generates the sequences

(7) $\cdots \rightarrow \mathbf{P}^1 \rightarrow -\mathbf{P}^2 \rightarrow -\mathbf{P}^1 \rightarrow \mathbf{P}^2 \rightarrow \mathbf{P}^1 \rightarrow \cdots$

The pattern coefficients $z_j$ in (2) are given as the dot product of $\mathbf{X}$ with the *adjoint patterns* $\mathbf{P}^A_j$, which are the normalized eigenvectors of $\mathfrak{A}^T$:

(8) $(\mathbf{P}^A_j)^T \mathbf{X} = \sum_k z_k \, (\mathbf{P}^A_j)^T \mathbf{P}_k = z_j$ , j=1,...,n.

All relationships derived to this point only depend on the existence of a linear equation (1) with some matrix $\mathfrak{A}$. No assumption has been made about the origin of this matrix. In dynamical theory, (1) is based on linearized and discretized differential equations. In the case of the POP analysis the relationship

(9) $\mathbf{X}(t+1) = \mathfrak{A} \cdot \mathbf{X}(t) + \textit{noise}$

is hypothesized. Multiplication of (9) from the right hand side by the transposed $\mathbf{X}(t)$ and taking expectations, $\mathcal{E}$, leads to

(10) $\mathfrak{A} = \mathcal{E}[\mathbf{X}(t+1)\mathbf{X}^T(t)] \cdot \left[\mathcal{E}[\mathbf{X}(t)\mathbf{X}^T(t)]\right]^{-1}$

which minimizes the noise term in (9) in the least squares sense. In practical situations, the lag-1 covariance matrix $\mathfrak{r}_1 = \mathcal{E}[\mathbf{X}(t+1)\mathbf{X}^T(t)]$ and the covariance matrix $\mathfrak{r}_0 = \mathcal{E}[\mathbf{X}(t)\mathbf{X}^T(t)]$ appearing in (10) have to be estimated from the data.The eigenvectors of (10), or, the normal modes of (9) are called *Principal Oscillation Patterns*. The time coefficients $z(t)$ are called *POP coefficients*. Their time evolution is given by (omitting again the index)

(11) $z(t+1) = \lambda \cdot z(t) + \textit{noise}$

Note that no reduction of the dimension of the problem is incorporated into the POP method itself. Therefore, in order to apply the POP analysis to systems with many (spatial) degrees of freedom, the data are often subjected to a truncated EOF expansion, and the POP analysis is applied to the vector of the first few EOF coefficients only. A positive by-product of this procedure is that in this way noisy components can be excluded from the analysis.

The stationarity of **X** together with (11) requires $\rho \leq 1$. The auto-spectrum $\Gamma_z$ of $z(t)$ is a function of the eigenvalue $\lambda$ and of the auto-spectrum $\Gamma_n$ of the noise:

$$\Gamma_z(\omega) = \frac{\Gamma_n(\omega)}{|e^{i\omega} - \lambda|^2} \tag{12}$$

The eigenvalue $\lambda = \rho exp(i\eta)$ is representative of the temporal statistics of the signal if the noise spectrum $\Gamma_n$ is almost white, i.e., $\Gamma_n(\omega) \approx$ constant. It is assumed for the remainder of this subsection that $\Gamma_n(\omega) = 1$.
The width of the spectrum depends on $\rho$. The smaller $\rho$ is, the broader is the spectrum. In the limit of $\rho = 0$ the spectrum is white. For each $\rho$ the spectrum $\Gamma_z$ has a single maximum $\Gamma_z = (1-\rho)^{-2}$ at $\omega = \eta$. If $\lambda$ is complex then $\eta \neq 0$. If $\lambda$ is real then $\eta = 0$, and the spectrum is red.

Thus, the POP analysis yields a multivariate spectral analysis of a vector time series (Hasselmann, 1988). A first attempt to simultaneously derive several signals with different spectra from a high dimensional data set is given by Xu (1991b).

## 3. EXAMPLES

### a) Tropospheric Rossby waves, given by POP analysis and stability analysis

In an attempt to identify tropospheric baroclinic waves a POP analysis with twice-daily geopotential heights at various tropospheric levels and a conventional linear stability analysis of the quasi-geostrophic vorticity equation was performed (Schnur et al., 1991). For both analyses the signals are expected to propagate mostly in the zonal direction on top of a zonally symmetric mean state. Therefore waves may conveniently be described in a semi-spectral representation either by cosine- and sine Fourier coefficients or by an amplitude and a phase.

In the *POP analysis*, the state vector $\mathbf{X}$ is formed from the data for each wave-number separately by the trigonometric coefficients of geopotential height at all latitudes and heights. Since $\mathbf{X}$ is formed by the sine- and cosine coefficients of the zonal geopotential height waves, both the real and the imaginary part of the complex POP, $\mathbf{P} = \mathbf{P}^1 + i\mathbf{P}^2$, represent a vector of sine- and cosine coefficients, too. They can be represented by amplitude patterns $\mathbf{A}^1$ and $\mathbf{A}^2$ and phase patterns $\Xi^1$ and $\Xi^2$.

The system matrix $\mathfrak{A}$ of (1) is estimated from ECMWF analyses for the winters (DJF) 1984/85 through 1986/87. There is a preconception of the time scale, so the analysed time series are band-pass filtered retaining all variability between 3 and 25 days.

Here, only one POP obtained for zonal wave number 8 of the Northern Hemisphere is discussed. The POP explains 54% of the wave number 8 variance, has a period $T$ of 4.0 days and a damping time of 8.1 days. Note that the decay time is sensitive to the type of time-filter. The amplitude and phase patterns of the POPs are shown in Figure 1 as height-latitudinal distributions. The amplitude fields $\mathbf{A}^1$ and $\mathbf{A}^2$, of $\mathbf{P}^1$ and $\mathbf{P}^2$, are almost identical, and the phase distribution $\Xi^1$ is shifted by about 90° eastward relative to the phase distribution $\Xi^2$ at those latitudes where the amplitudes are significant. This information, together with the interpretation (7) leads to the conclusion that this POP describes an eastward travelling wave.

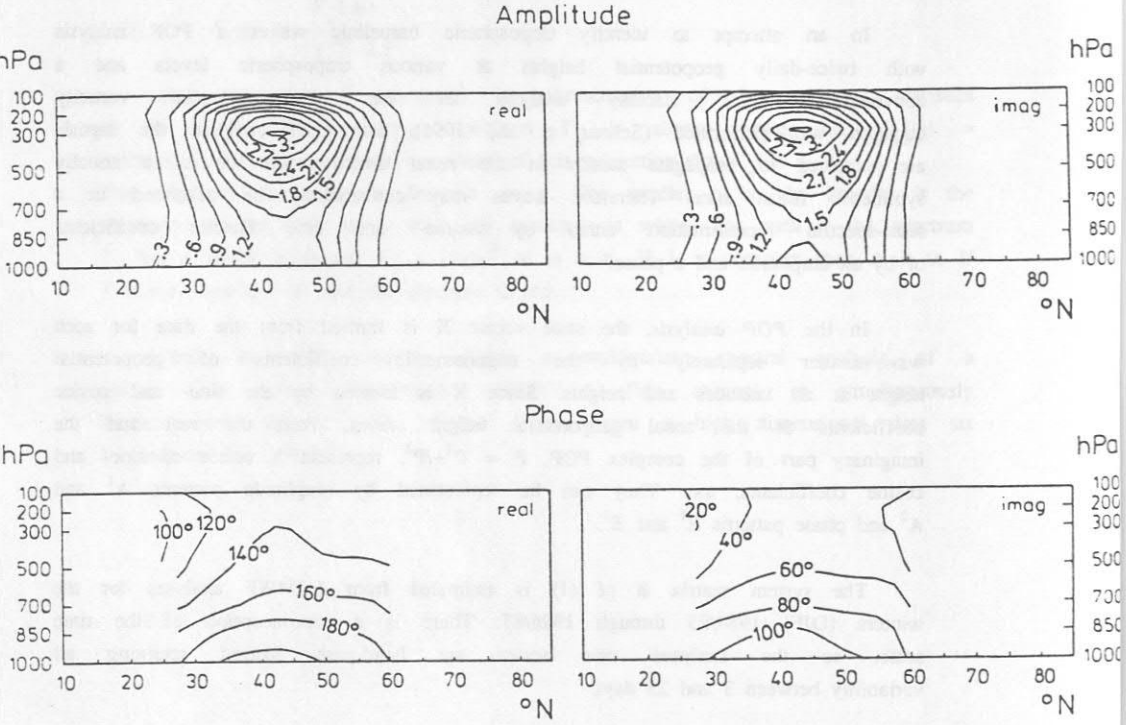


**Figure 1**

Baroclinic waves: The patterns $\mathbf{P}^1$ and $\mathbf{P}^2$ of a POP analysis of twice-daily geopotential height for zonal wave-number 8. The data have been filtered so that only variance between 3 and 25 days is retained. The analysis is made for the Northern hemisphere and for the three winters (DJF) 1984 to 1987. The oscillation period $T$ is 4 days, and the e-folding time is 8.6 days.

Since the analysis is done in wave-number space, the analysed time series $\mathbf{X}$ consists of the sine and cosine coefficients at all levels and latitudes. Thus the two patterns $\mathbf{P}^1$ and $\mathbf{P}^2$ can be both represented by amplitude patterns $\mathbf{A}^1$ and $\mathbf{A}^2$ (top) and phase patterns $\Xi^1$ and $\Xi^2$ (bottom).

(From Schnur et al., 1991)

Cross spectral analysis of the coefficient time series $z^1(t)$ and $z^2(t)$ reveals maximum variance at time scales of 3 to 5 days, an almost uniform phase difference of $90^0$, as it should, and very high coherence in the neighborhood of the POP period of 4 days (not shown).

In the *stability analysis* the system matrix $\mathfrak{A}$ is derived from the discretized quasi-geostrophic vorticity equation on a sphere linearized around the observed zonally averaged mean winter state. The eigenvectors of this $\mathfrak{A}$ are the *normal modes* of the quasi-geostrophic vorticity equation. These modes $\mathbf{Q} = \mathbf{Q}_1 + i\mathbf{Q}_2$ are complex and invariant against zonal displacements since $\mathfrak{A}$ is derived from a zonally averaged basic state. Therefore, $\mathbf{Q}^1$ and $\mathbf{Q}^2$ coincide except for a phase difference of $90^\circ$ so that $\mathbf{Q}$ represents a zonally propagating wave.

The most unstable normal mode obtained for wave-number 8 of the Northern hemi-sphere has a period is $T$ = 3.9 days. It is amplifying so that an initial amplitude is doubled after 1.5 days. The mode is propagating eastward. Its amplitude pattern $\mathbf{A}^q$ (Fig. 2) is almost identical to the amplitude patterns of the POP shown in Fig. 1: $\mathbf{A}^q \approx \mathbf{A}^1 \approx \mathbf{A}^2$. A difference is the maximum of the normal mode at the bottom which can be attributed to the omission of friction in the stability analysis. The phase pattern $\Xi^q$ has the same structure as the POP phases.

The normal mode coefficients $z_1(t)$ and $z_2(t)$ explain 38% of the wave number 8 variance. The cross-spectrum between $z_1(t)$ and $z_2(t)$ (not shown) is similar to the cross-spectrum of the POP coefficients. Also, a complex cross-spectral analysis between the POP coefficients and the coefficients of the unstable mode shows that both time series are highly coherent at periods of about 4 days.

Summarizing, the POP analysis which estimates the system matrix of a linear system from observational data finds similar modes as a conventional stability analysis which makes use of first-principle dynamical reasoning to obtain the matrix. Thus, the POP patterns can be attributed to the linear growing phase in the life cycle of baroclinic waves.

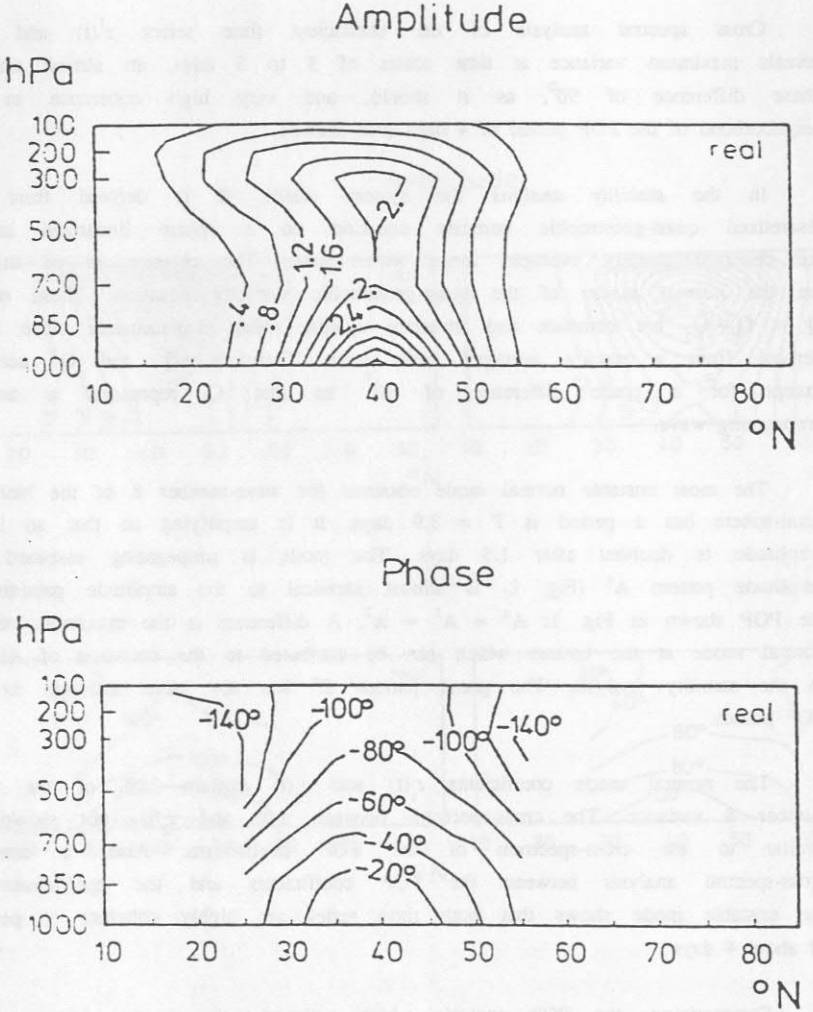


**Figure 2**

Baroclinic waves: The patterns $Q^1$ and $Q^2$ of the most unstable zonal wave-number 8 mode on the Northern hemisphere identified in stability analysis of the discretized quasi-geostrophic vorticity equation linearized about the observed zonal mean state in northern winter. The growth rate is 2.2 days (i.e. an initial amplitude is amplified by a factor of $e$ in 2.2 days), and the period $T$ is 3.9 days.

Since the unstable mode is completely determined by the real part only the amplitude and phase pattern $A^q$ and $\Xi^q$ of $Q^1$ have to be shown. $Q^2$ is then given by $A^q$ and $\Xi^q - \pi/2$.

(From Schnur et al., 1991)

**b) The Southern Oscillation and the Quasi-Biennial Oscillation**

Two oscillations in the tropical atmosphere with similar oscillation period - the stratospheric *Quasi-Biennual Oscillation* QBO and the tropospheric Southern Oscillation (SO) - and the relationship between these two oscillations, are examined using the POP analysis (Xu, 1991a).

The QBO is reflected in observations of equatorial zonal wind in the strato-sphere. Monthly mean anomalies along the equator (50°E - 80°W) of 10m zonal wind and of sea-surface temperature (SST) anomalies are used to describe the SO-signal. To remove high frequency noise from the surface data the time series are low-pass filtered. The stratospheric data are unfiltered. The three data sets - stratospheric wind and SO-related zonal surface wind and SST - are simultaneously "POP analyzed". The three components are normalized so that they contribute the same variance to the combined data set.

Two significant POP pairs are found, one with an oscillation period $T$ = 28 months, the other with $T$ = 45 months. Cross-spectral analysis of the POP coefficients (not shown) indicates that the 28 month period is reliably estimated, but that the period $T$ = 45 months is overestimated. A more adequate period would be 30 months or so.

The patterns of the two modes are shown in Fig. 3. The first mode is significant only in the stratosphere where it represents the downward propagation of a signal from the uppermost level to the lower stratosphere within 14 months. The time series of POP coefficients (not shown) oscillates regularly and has a torus-shaped distribution in phase space (Fig. 4a). The second mode is significant only in the surface-wind and in the SST. The mode describes an eastward propagation, from the Indian Ocean into the Pacific Ocean, in the surface-wind, and a almost standing feature in the SST. Sometimes the POP coefficient time series oscillate regularly, and the occurrence of El Niño and La Niña-events is closely related to these oscillatory intervals. When the Southern Oscillation is quiet, the POP coefficients are small and noisy. The distribution of the POP coefficients in phase space (Fig. 4b) is almost bivariate normal.

The two POPs of the combined data sets represent the QBO and the SO. The correlations between the POP coefficient time series of the two modes are negligibly small. We conclude that the two modes are identified as being, to first order approximation, statistically independent.

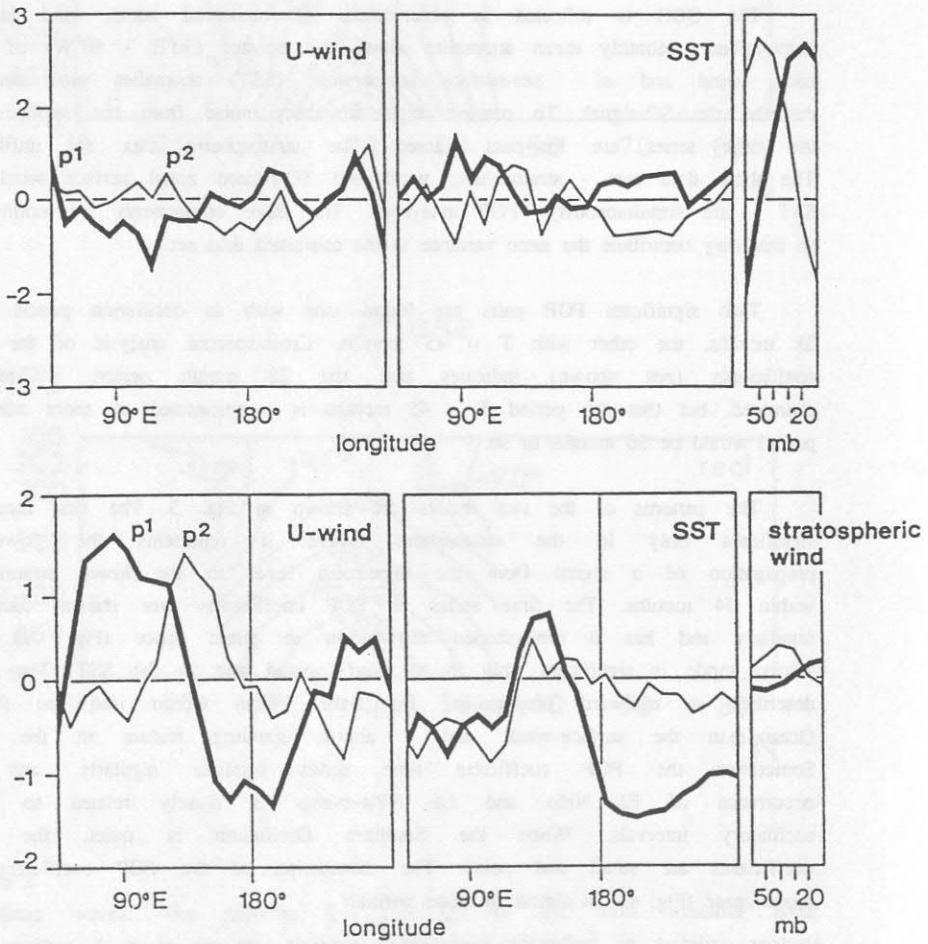


**Figure 3**

QBO and SO: POP patterns $P^1$ and $P^2$ from

b) the first mode, representing the QBO, of the POP analysis for the combined data set that includes the stratospheric zonal wind and surface zonal wind and SST anomalies.

b) the second mode, representing the SO, of the POP analysis for the combined data set that includes the stratospheric zonal wind and surface zonal wind and SST anomalies.

(from Xu, 1991)

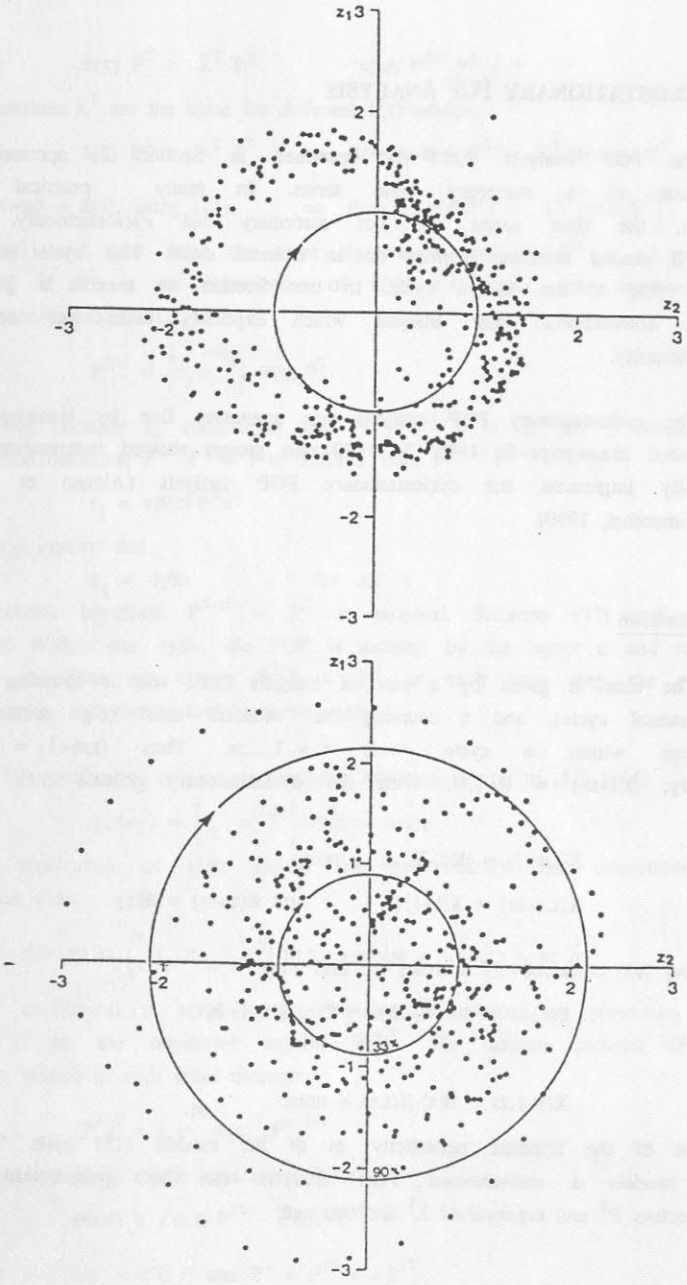


Figure 4

QBO and SO: Distributions of the complex POP coefficients connected with the patterns shown in Figure 4.

a) The coefficients of the first mode, representing the QBO.

a) The coefficients of the second mode, representing the SO.

(From Xu, 1991)

## 4. CYCLOSTATIONARY POP ANALYSIS

The POP analysis that was described in Section 2, operates on the assumption of a stationary time series. In many practical situations, however, the time series are not stationary but *cyclostationary*, i.e., the first and second moments depend on an external cycle. This cycle is often the annual cycle or the diurnal cycle. In this Section we present a generalization of the conventional POP analysis which explicitly takes into account this non-stationarity.

The cyclostationary POP analysis was suggested first by Hasselmann in an unpublished manuscript in 1985. In 1990 two groups showed independently how to practically implement the cyclostationary POP analysis (Alonso et al., 1991; and Blumenthal, 1990).

### a) Definition

The time is given by a pair of integers $(t,\tau)$, with $t$ counting the cycles (e.g, annual cycle), and $\tau$ counting the "seasonal date" (e.g. month), i.e. the time-steps within a cycle, with $\tau = 1,...,m$. Thus $(t,m+1) = (t+1,1)$ or, generally, $(t,\tau+m) = (t+1,\tau)$. Then the cyclostationary process may be written as

$$\mathbf{X}(t,\tau+1) = \mathfrak{A}(\tau)\cdot\mathbf{X}(t,\tau) + \text{noise} \tag{13}$$

with $\mathbf{X}(t,\tau+m) = \mathbf{X}(t+1,\tau)$ and $\mathfrak{A}(\tau+m) = \mathfrak{A}(\tau)$

Applying (13) consecutively m-times we find with

$$\mathfrak{B}(\tau) = \mathfrak{A}(\tau+m-1)\cdot\mathfrak{A}(\tau+m-2)\cdot\ldots\mathfrak{A}(\tau+1)\cdot\mathfrak{A}(\tau) \tag{14}$$

that

$$\mathbf{X}(t+1,\tau) = \mathfrak{B}(\tau)\cdot\mathbf{X}(t,\tau) + \text{noise} \tag{15}$$

Because of the imposed periodicity, m of the models (15) exist. To each of these models a conventional POP analysis can be applied. In this way eigenvectors $\mathbf{P}^\tau$ and eigenvalues $\lambda^\tau$ are obtained:

$$\mathcal{B}(\tau)\ \mathbf{P}^{\tau} = \lambda^{\tau}\ \mathbf{P}^{\tau} \qquad \text{with } \mathbf{P}^{\tau T *}\cdot\mathbf{P}^{\tau} = 1$$

The eigenvalues $\lambda^{\tau}$ are the same for different $\mathcal{B}(\tau)$-models:

$$\mathcal{B}(\tau)\ \mathbf{P}^{\tau} = \lambda^{\tau}\ \mathbf{P}^{\tau} \quad \Rightarrow \quad \mathcal{A}(\tau+m)\cdot\mathcal{B}(\tau)\ \mathbf{P}^{\tau} = \lambda^{\tau}\ \mathcal{A}(\tau+m)\cdot\mathbf{P}^{\tau}$$

Since $\mathcal{A}(\tau+m) = \mathcal{A}(\tau)$, using (14): $\quad \Rightarrow \quad \mathcal{B}(\tau+1)\cdot\left[\mathcal{A}(\tau)\mathbf{P}^{\tau}\right] = \lambda^{\tau}\left[\mathcal{A}(\tau)\cdot\mathbf{P}^{\tau}\right]$.

Thus $\mathcal{B}(\tau+1)$ and $\mathcal{B}(\tau)$ share the same eigenvalues, and $\mathcal{A}(\tau)\cdot\mathbf{P}^{\tau}$ is an eigenvector of $\mathcal{B}(\tau+1)$ if $\mathbf{P}^{\tau}$ is an eigenvector of $\mathcal{B}(\tau)$. Of course, the eigenvectors are subject to normalization, i.e.,

(16) $$\mathbf{P}^{\tau+1} = \left(r_{\tau}\cdot e^{i\phi_{\tau}}\right)\ \mathcal{A}(\tau)\cdot\mathbf{P}^{\tau}$$

with a real constant $r_{\tau}$ chosen so that $[\mathbf{P}^{\tau}]^{T*}\cdot\mathbf{P}^{\tau} = 1$. If, for a certain $\tau$, the normalization condition $\mathbf{P}^{\tau T *}\cdot\mathbf{P}^{\tau} = 1$ is fulfilled, then $\mathbf{P}^{\tau+1 T *}\cdot\mathbf{P}^{\tau+1} = 1$ if

(17) $$r_{\tau} = \|\mathcal{A}(\tau)\cdot\mathbf{P}^{\tau}\|^{-1}$$

With $\lambda = \rho\ exp(i\eta)$ and

(18) $$\phi_{\tau} = -\eta/m \qquad \text{for all } \tau$$

the periodicity condition $\mathbf{P}^{\tau+m} = \mathbf{P}^{\tau}$ is satisfied. Relation (17) and (18) are reasonable: Within one cycle, the POP is damped by the factor $\rho$ and rotated by an angle $\eta$. Thus, to ensure $\mathbf{P}^{\tau+m} = \mathbf{P}^{\tau}$, at each time step the pattern is amplified by $r_{\tau}$ and rotated backwards by $-\eta/m$.

For the POP coefficients $z(t)$ a time evolution equation similar to (15) holds:

(19) $$z(t,\tau+1) = \left(r_{\tau}^{-1}\ e^{i\eta/n}\right)\cdot z(t,\tau) + \textit{noise}$$

Repeated application of (19) yields, not unexpectedly, the conventional POP model result (15):

$$z(t+1,\tau) = \left(\prod_{k=0}^{m-1} r_{\tau+k}\right)^{-1} e^{i\eta}\cdot z(t,\tau) + \textit{noise} = \lambda\cdot z(t,\tau) + \textit{noise}$$

The time coefficients at a given time t may be obtained by projecting the full field $\mathbf{X}(t,\tau)$ on the respective adjoint $[\mathbf{P}^{A}]^{\tau}$. The adjoint patterns $[\mathbf{P}^{A}]^{\tau}$ and $[\mathbf{P}^{A}]^{\tau+1}$ are related to each other through:

(20) $$[\mathbf{P}^{A}]^{\tau} = r_{\tau}\cdot e^{i\phi}\cdot\mathcal{A}(\tau)^{T}[\mathbf{P}^{A}]^{\tau+1}$$

The contribution $\mathbf{p}(t,\tau)$ to the time series $\mathbf{X}(t,\tau)$ is

(21) $$\mathbf{p}(t,\tau) = z^{1}(t,\tau)\cdot\mathbf{P}^{1\tau} - z^{2}(t,\tau)\cdot\mathbf{P}^{2\tau}$$

with $2z(t,\tau) = z^{1}(t,\tau) + iz^{2}(t,\tau)$ and $\mathbf{P}^{\tau} = \mathbf{P}^{1\tau} + i\cdot\mathbf{P}^{2\tau}$

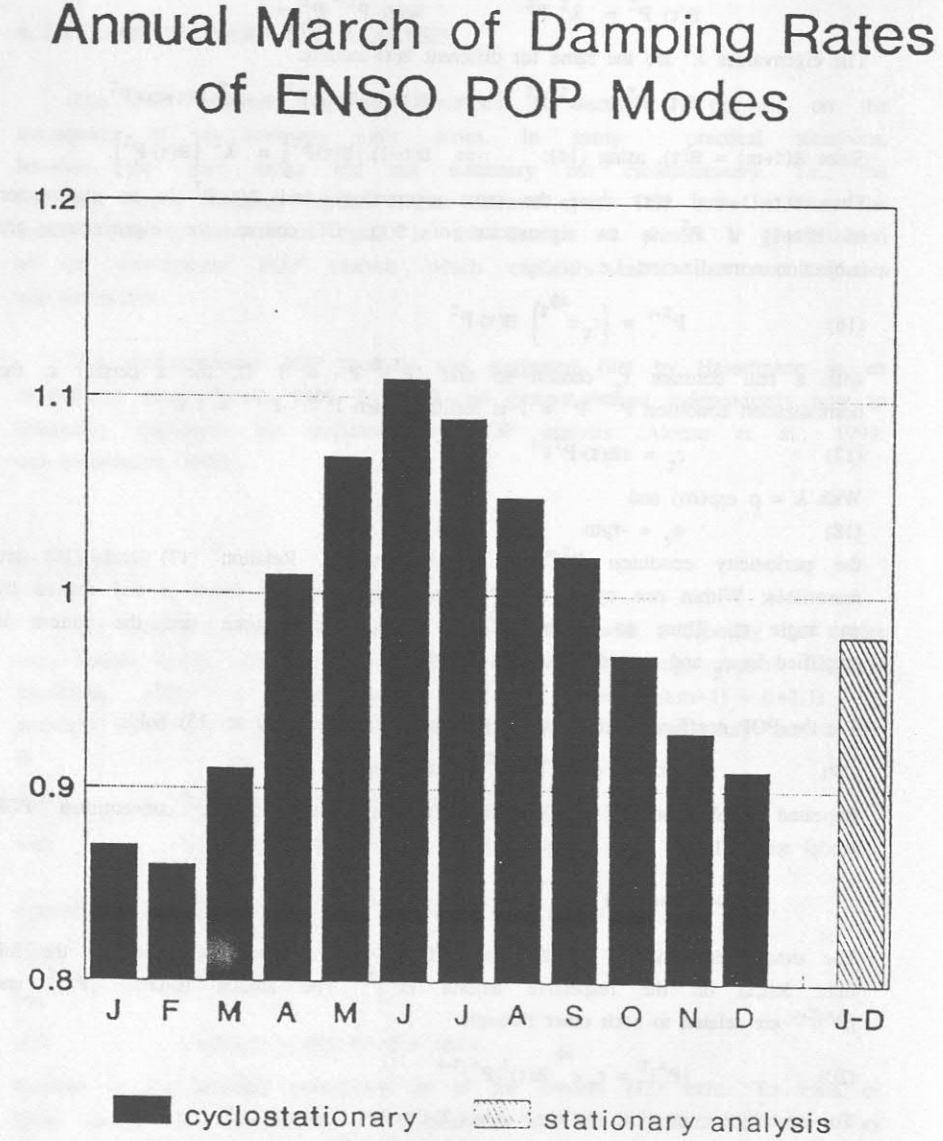


**Figure 5**

ENSO: Damping rates obtained in the stationary POP analysis and in the cyclostationary POP analysis of the Southern Oscillation (in terms of equatorial zonal surface-wind and SST). For the stationary analysis one damping rate, representing the average damping from one months to the next, is shown. In the cyclostationary analysis a separate damping rate is obtained for each month.

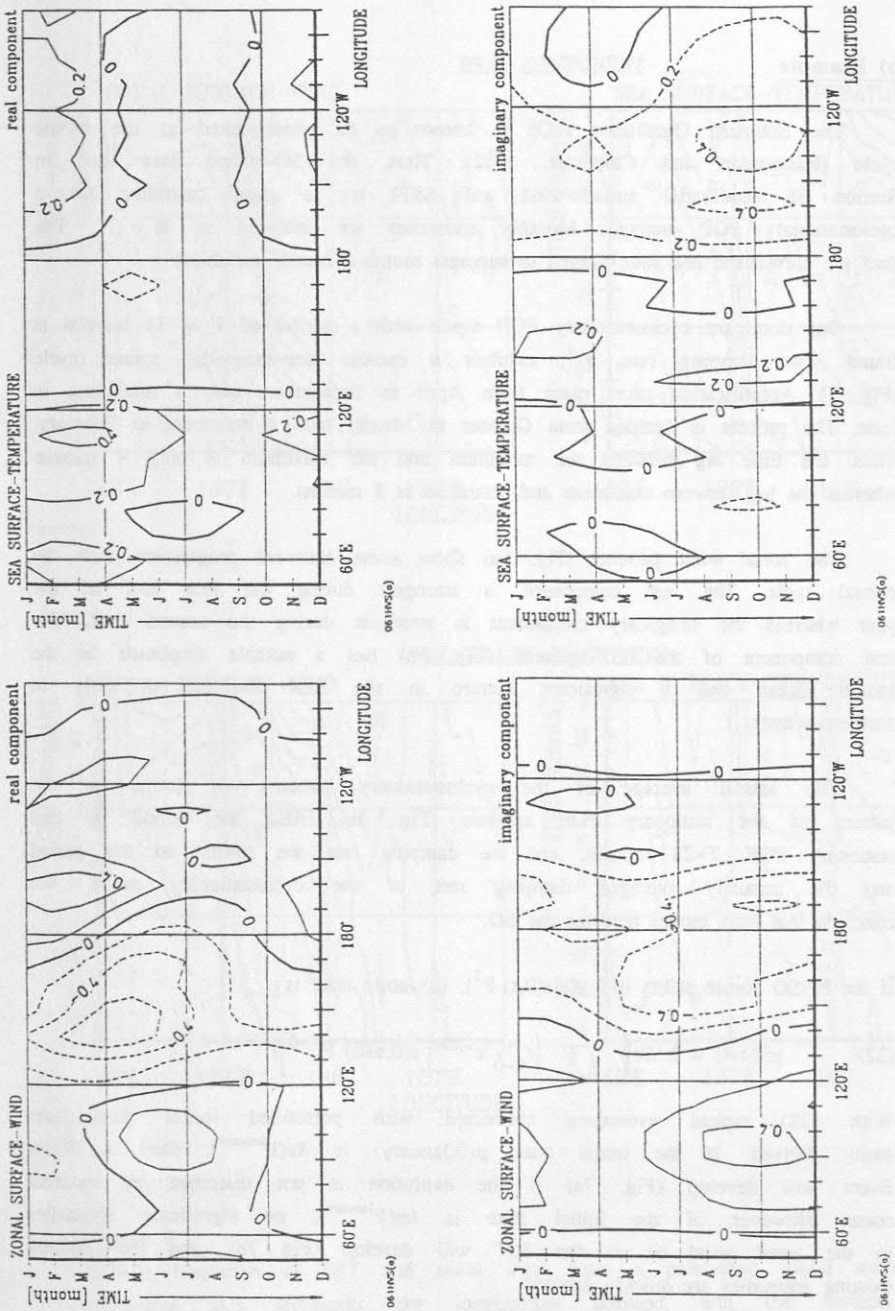


**Figure 6**

ENSO: Cyclo-stationary POPs of the combined normalized band-pass filtered zonal wind/SST data set. The horizontal axis represents longitude along the equator, and the vertical axis the annual cycle of the patterns.

a) The zonal wind patterns.

b) The SST patterns.

**b) Example**

The Southern Oscillation (SO) is known to be phase-locked to the annual cycle (Rasmusson and Carpenter, 1982). Thus, the SO-related data used in Section 3b (equatorial surface-wind and SST) are a good candidate for a cyclostationary POP analysis. Monthly anomalies are analysed so m = 12. The data are normalized and time-filtered to suppress month-to-month variability.

One dominant cyclostationary POP mode with a period of $T$ = 31 months is found. The damping rate, $r_\tau^{-1}$, exhibits a marked non-sinusoidal annual cycle (Fig. 5). Amplification takes place from April to September, with a maximum in June. The process is damped from October to March, with a minimum in February. Thus, the time lag between the minimum and the maximum is only 4 months whereas the lag between maximum and minimum is 8 months.

The *zonal wind* patterns (Fig. 6a) show some eastward progression with the annual cycle. The real component is strongest during the first half of the year whereas the imaginary component is strongest during the second half. The real component of the *SST* pattern (Fig. 6b) has a notable amplitude in the Indian Ocean and a significant feature in the East Pacific, but only in northern winter.

The annual average of the cyclostationary patterns is similar to the pattern of the stationary POP analysis (Fig. 3b). Also the period of that stationary POP, $T$=28 months, and the damping rate are similar to the period and the annually averaged damping rate of the cyclostationary mode. We conclude that both modes describe the SO.

If the ENSO signal $\mathbf{p}(0,\tau)$ is $2\ Re[z(0,\tau)\cdot\mathbf{P}^{\tau}]$, its future state is

$$\mathbf{p}(0,t+t) = 2\ Re\left[\prod_{\delta=1}^{t}\left(r_{\tau+\delta}^{-1}\, e^{i\eta/n}\right)\cdot z(0,\tau+\delta)\ \mathbf{P}^{\tau+\delta}\right] \qquad (22)$$

With (22) typical evolutions connected with prescribed initial states are easily derived. If the initial state $\mathbf{p}$(0,January) is $Re(\mathbf{P}^{January})$, then a Warm Event will develop (Fig. 7a) if the evolution is not disturbed by external noise. However, if the initial state is $Im(\mathbf{P}^{January})$, no significant anomalies in the zonal wind or in the SST will develop (Fig 7b), and the initially existing anomalies are quickly damped.

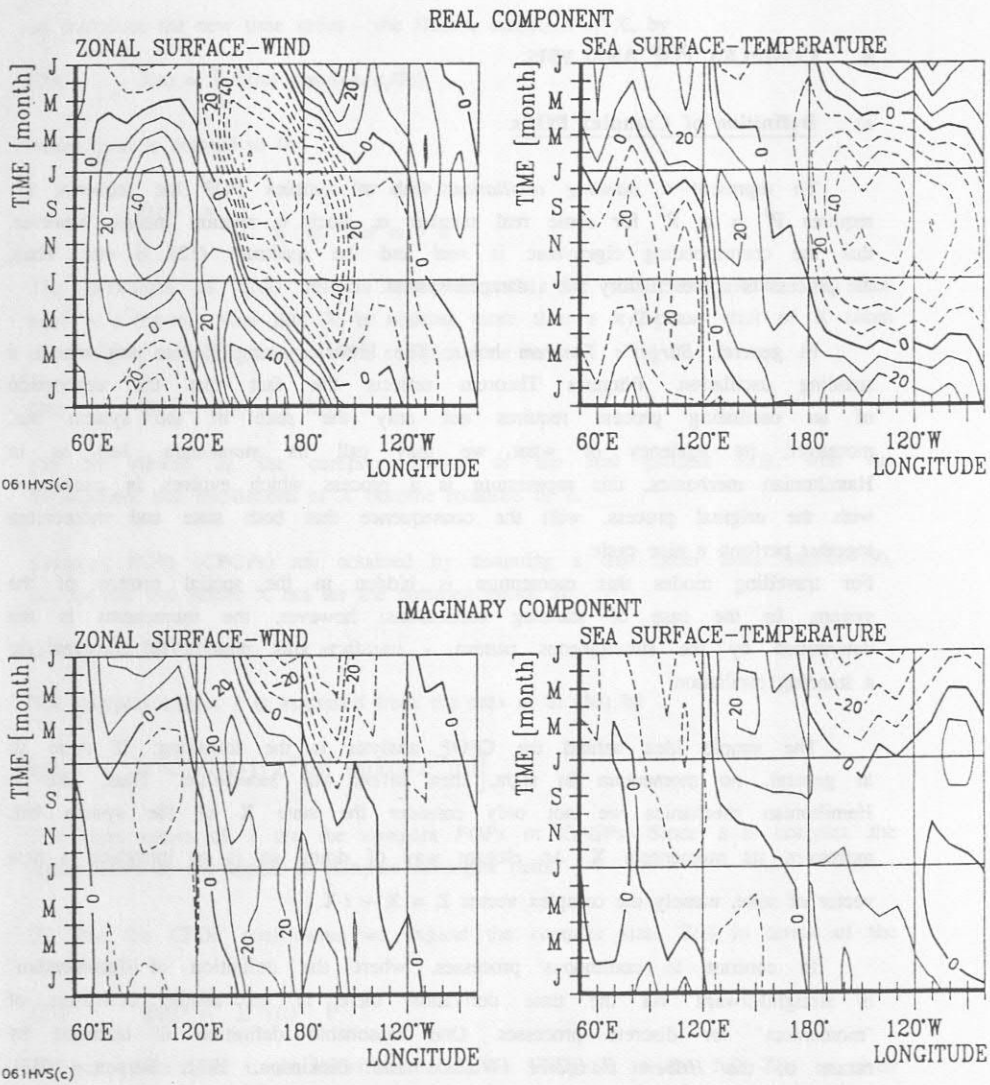


**Figure 7**

ENSO: Evolution of SST and zonal wind from a prescribed initial state. The horizontal axis represents the longitudinal position, and the vertical axis represents in the downward direction a 24-month time interval.

a) Initial state in January is the real component of POP.

b) Initial state in January is the imaginary component of POP.

# 6. COMPLEX POP ANALYSIS

## a) Definition of Complex POPs

To represent a *standing oscillation* with a complex POP the sequence (7) requires $\mathbf{P}^1 = \alpha\ \mathbf{P}^2$ for some real number $\alpha$. Such a relation means, however, that the corresponding eigenvalue is *real* and the spectrum (12) is red. Thus, the process is not oscillatory but a damped system.

In general, *Bürger's Theorem* holds: The linear system (1) can not model a standing oscillation. Bürger's Theorem reflects the fact that the description of an oscillating process requires not only the state of the system but, moreover, its tendency or what we may call its *momentum*. Just as in Hamiltonian mechanics, this momentum is a process which evolves *in quadrature* with the original process, with the consequence that both state and momentum together perform a nice cycle.
For travelling modes this momentum is hidden in the spatial pattern of the system. In the case of standing oscillations, however, the momentum is not determined by the simultaneous pattern - in fact this pattern is constant for a standing oscillation.

The simple idea behind the CPOP analysis is the following: If there is, in general, no momentum in sight, then *invent this momentum!* Thus, like in Hamiltonian mechanics we not only consider the state $\mathbf{X}$ of the system but, moreover, its momentum $\dot{\mathbf{X}}$. An elegant way of doing so is to introduce a new vector of state, namely the complex vector $\mathbf{Z} = \mathbf{X} + i\cdot\dot{\mathbf{X}}$.

In contrast to continuous processes, where the definition of "momentum" is straightforward via the time derivation there is no unique definition of "momentum" for discrete processes. One reasonable definition is obtained by means of the *Hilbert transform* (Wallace and Dickinson, 1972; Barnett, 1983): If X(t) is a real time series with Fourier decomposition

$$X(t) = \sum_{\omega} x(\omega)\ exp(i\omega t)$$

we introduce the new time series - the *Hilbert transform of* X, by

$$\dot{X}(t) = \sum_{\omega} \xi(\omega)\ exp[i(\omega t+\pi/2)] \quad , \tag{23}$$

where $\xi(\omega)$ is defined to be

$$\xi(\omega) = \begin{cases} x(\omega) & \text{for } \omega \le \pi \\ x^{*}(\omega) & \text{for } \omega > \pi \end{cases} \quad .$$

The definition of $\xi(\omega)$ reflects the fact that for real time series one has $x(\omega) = x^{*}(2\pi-\omega)$. Note that $\dot{X}$ is nothing more than a $\pi/2$-phase shift of X taken uniformly at each frequency $\omega$. The complex time series

$$Z(t) = X(t) + i\cdot \dot{X}(t) \quad . \tag{24}$$

can be viewed as the complex analog of the real process X(t), with the consequence that oscillations of X become rotations of Z.

Complex POPs (CPOPs) are obtained by assuming a first order linear model (9), not for the real vector X but for the complex vector **Z**:

$$\mathbf{Z}(t+1) = \mathfrak{Z} \cdot \mathbf{Z}(t) + \textit{noise} \tag{25}$$

The complex matrix $\mathfrak{Z}$ is estimated from the data as in (10) by

$$\mathfrak{Z} = \mathcal{E}(\mathbf{Z}(t+1)\cdot\mathbf{Z}^{T^{*}}(t)) \left[\mathcal{E}(\mathbf{Z}(t)\cdot\mathbf{Z}^{T^{*}}(t))\right]^{-1} \tag{26}$$

The eigenvectors of $\mathfrak{Z}$ are the *complex POPs* or *CPOPs*. Since $\mathfrak{Z}$ is complex the eigenvectors do not appear in complex conjugate pairs.

To find the CPOP coefficients we expand the *complex* state $\mathbf{Z}(t)$ in terms of the CPOP basis

$$\mathbf{Z}(t) = \sum_{j} \gamma_{j}(t) \cdot \mathbf{P}_{j} \quad . \tag{27}$$

At any given time t, the contribution of the CPOP **P** to the full $\mathbf{Z}(t)$ is given by the complex process $\mathbf{p}(t) = \gamma(t)\cdot\mathbf{P}$, or, with $\mathbf{p} = \mathbf{p}^{1}+i\cdot\mathbf{p}^{2}$, $\mathbf{P} = \mathbf{P}^{1}+i\cdot\mathbf{P}^{2}$ and $\gamma = \gamma^{1}+i\cdot\gamma^{2}$

$$\mathbf{p}^{1}(t) = \gamma^{1}(t)\cdot\mathbf{P}^{1} - \gamma^{2}(t)\cdot\mathbf{P}^{2} \tag{28}$$

(29) $\mathbf{p}^2(t) = \gamma^1(t)\cdot\mathbf{P}^2 + \gamma^2(t)\cdot\mathbf{P}^1$

The real part $\mathbf{p}^1(t)$ describes the signal in the "location" $\mathbf{X}$-space whereas the imaginary part $\mathbf{p}^2(t)$ describes the signal in the "momentum" $\dot{\mathbf{X}}$-space. Without noise the temporal evolution of the CPOP coefficient $\gamma$ is given by (4) so that (28,29) are equivalent to

(30) $\mathbf{p}^1(t) = \rho^1(\cos(\eta t)\cdot\mathbf{P}^1 - \sin(\eta t)\cdot\mathbf{P}^2)$

(31) $\mathbf{p}^2(t) = \rho^1(\cos(\eta t)\cdot\mathbf{P}^2 + \sin(\eta t)\cdot\mathbf{P}^1)$

with $\lambda = \rho\cdot exp(i\eta)$. Hence, the typical evolution is

$$
\begin{array}{l}
\cdots \rightarrow \mathbf{P}^1 \rightarrow -\mathbf{P}^2 \rightarrow -\mathbf{P}^1 \rightarrow \mathbf{P}^2 \rightarrow \mathbf{P}^1 \rightarrow \cdots \text{ in the "location" } \mathbf{X}\text{-space,} \\
\qquad\quad | \qquad | \qquad | \qquad | \qquad | \\
\cdots \rightarrow \mathbf{P}^2 \rightarrow \mathbf{P}^1 \rightarrow -\mathbf{P}^2 \rightarrow -\mathbf{P}^1 \rightarrow \mathbf{P}^2 \rightarrow \cdots \text{ in the "momentum" } \dot{\mathbf{X}}\text{-space.}
\end{array}
\tag{32}
$$

**b) Example: El Niño - Southern Oscillation**

In Section 3b and 4b equatorial surface data were analysed in order to isolate the SO signal. In the low-pass filtered data set the SO signal was identified as a travelling pattern in the zonal wind and as a standing pattern in the SST.

We applied the CPOP model (25) to the unfiltered equatorial (50°E to 80°W) SST data set and found one dominant CPOP with a period of 39 months and damping time of 36 months. The $\mathbf{P}^1$-pattern is positive almost everywhere, with a primary maximum in the Pacific Ocean and a secondary maximum in the Indian Ocean (Fig. 8a). $\mathbf{P}^2$ is nearly zero over the whole Pacific Ocean, and symmetric to $\mathbf{P}^1$, i.e. negative, in the Indian Ocean. The CPOP coefficients vary coherently (Fig. 8b) and share a correlation coefficient of 74% with the Southern Oscillation Index (SOI). So the cycles (32) indicate that the signal is a standing oscillation, with a period of 39 months over the Pacific Ocean and one of $39/2 \approx 20$ months over the Indian Ocean (see Fig. 8a).

The POP analysis revealed useful patterns only after the data were band-pass filtered. Then a complex pair was obtained with a pattern and period almost the same as those of the CPOP but with coefficients that vary

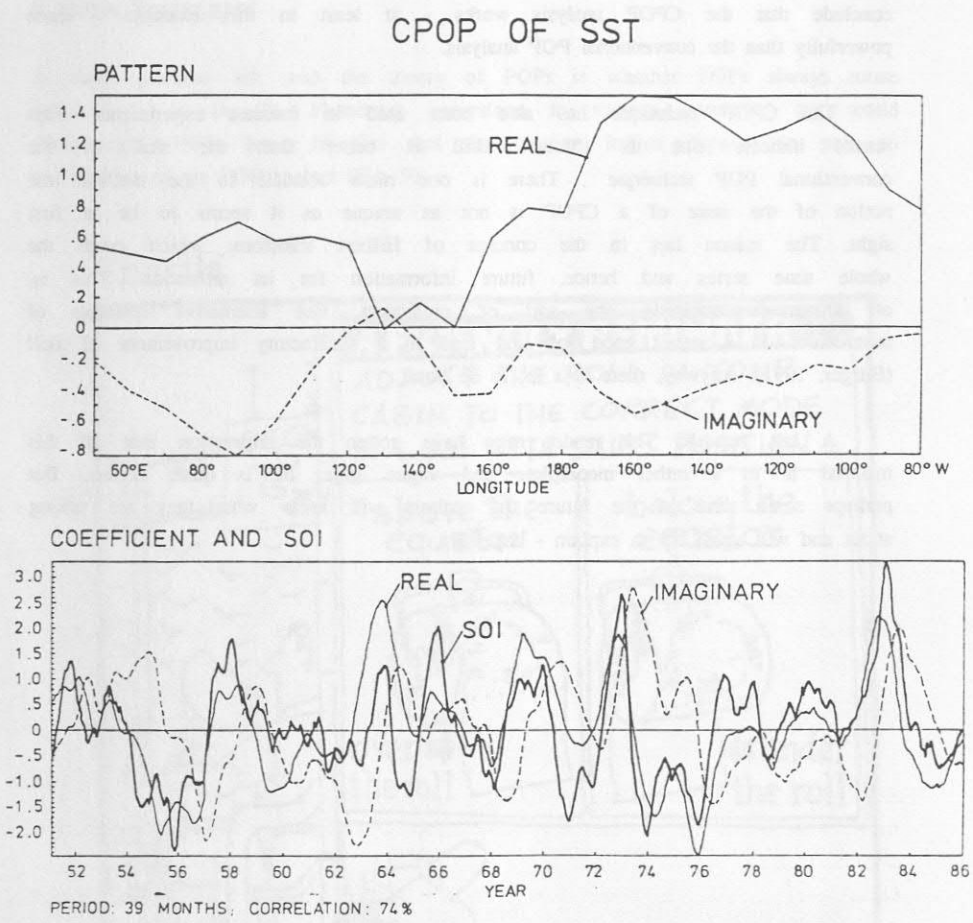


**Figure 8**

ENSO: The dominant mode identified in a complex POP analysis of equatorial SST. The period is 39 months, the damping time 36 months.

a) The patterns (compare with Fig. 3b and 6b)

b) CPOP coefficients and the Southern Oscillation Index.

(after Bürger, 1991)

incoherently and which show a rather low correlation of 44% to the SOI. We conclude that the CPOP analysis works - at least in this example - more powerfully than the conventional POP analysis.

The CPOP technique has also been used in forecast experiments. First results indicate that its forecast skill is better than the skill of the conventional POP technique . There is one main obstacle to the method: the notion of the *state* of a CPOP is not as unique as it seems to be at first sight. The reason lies in the concept of Hilbert transform which needs the whole time series and hence, future information for its definition. This is, of course, undermining any sort of prediction. But alternative concepts of momentum do a rather good job and lead to a satisfactory improvement of skill (Bürger, 1991). Anyway, there is a lot to be done.

A last remark: The reader may have gotten the impression that all this material is in a rather incomplete and vague state; he is quite correct. But perhaps some time in the future the authors will know what they are talking about and will again try to explain - hopefully.

## 6. Open Problems

A major problem left with the theory of POPs is whether POPs always rotate "clockwise", as in (7). Numerous excursions to various parts of the world (Weinberger, 1991) have revealed that the rotation indeed depends in part on the location of the POP analyst (Fig. 9).

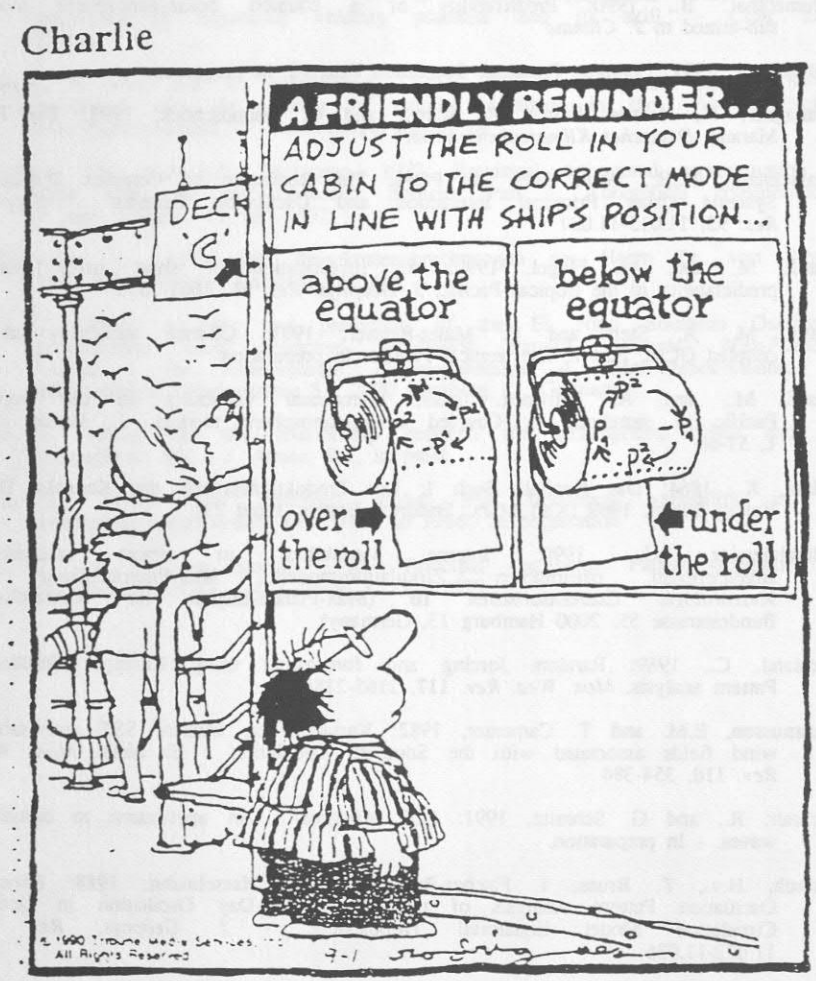


**Figure 9**

The location of the POP analyst and the rotation of the POPs.

## REFERENCES


Alonso, M., M.J. Ortiz and A. Ruiz de Elvira, 1991: Application of statistical techniques to the analysis and prediction of ENSO. Part I: Exploratory analysis. Part II: Cyclostationary dependence. Submitted to *J. Climate*

Barnett. T.P., 1983: Interaction of the monsoon and pacific trade wind systems at interannual time scales: Part I. The equatorial zone. *Mon. Wea. Rev.* 111, 756-773

Blumenthal, B., 1990: Predictability of a coupled ocean-atmosphere model. sub-mitted to *J. Climate*

Bürger, G., 1991: Complex Principal Oscillation Patterns. In preparation

Gallagher, F., H von Storch, R. Schnur and G. Hannoschöck, 1991: The POP Manual. *Deutsches Klimarechenzentrum*

Hasselmann, K..H., 1988: PIPs and POPs: The Reduction of Complex Dynamical Systems Using Principal Interaction and Oscillation Patterns. - *Geophys. Res.* **93**, 11.015-11.021

Latif, M. and, M. Flügel, 1990: An investigation of short range climate predictability in the tropical Pacific. *J. Geophys. Res.* **96**, 2661-2673

Latif, M., A. Sterl and E. Maier-Reimer, 1991: Climate variability in a coupled GCM. Part I: The tropical Pacific. In preparation

Latif, M., and A. Villwock, 1989: Interannual variability in the tropical Pacific as simulated in Coupled ocean-atmosphere models. *J. Marine Sys.* **1**, 51-60

Marx, K., 1864: Das Kapital. Buch I: Der Produktionsprozeß des Kapitals. Dietz Verlag Berlin, 1969 (Karl Marx, Friedrich Engels, Band 23)

Mikolajewicz, U., 1990: Interne Variabilitat in einem stochastisch angetriebenen ozeanischen Zirkulationsmodell. *Max-Planck-Institut für Meteorologie Examensarbeiten* **10** (Max-Planck-Institut für Meteorologie; Bundesstrasse 55; 2000 Hamburg 13, Germany)

Penland, C., 1989: Random forcing and forecasting using Principal Oscillation Pattern analysis. *Mon. Wea. Rev.* **117**, 2165-2185

Rasmusson, E.M. and T. Carpenter, 1982: Variations in tropical SST and surface wind fields associated with the Southern Oscillation / El Niño. *Mon. Wea. Rev.* **110**, 354-384

Schnur, R., and G. Schmitz, 1991: POP Analysis - An application to baroclinic waves. - In preparation.

Storch, H.v., T. Bruns, I. Fischer-Bruns and K. Hasselmann, 1988: Principal Oscillation Pattern Analysis of the 30- to 60-Day Oscillation in General Circulation Model Equatorial Troposphere. - *J. Geophys. Res.* **93**, 11.022-11.036

Storch, H. von, and J. Xu, 1990: Principal Oscillation Pattern Analysis of the tropical 30- to 60-day oscillation. Part I: Definition on an index and its prediction. - *Clim. Dyn.* **4**, 175-190

Storch, H. von; U. Weese and J. Xu, 1990: Simultaneous analysis of space-time variability: Principal Oscillation Patterns and Principal Interaction Patterns with applications to the Southern Oscillation. - *Z. Meteor.* **40**, 99-103

Storch, H. von, and D. Baumhefner, 1991: Principal Oscillation Pattern Analysis of the tropical 30- to 60-days oscillation. Part II: The prediction of equatorial velocity potential and its skill. - *Clim. Dyn.* **5**, 1-12

Storch, H. von, and A. Smallegange, 1991: The phase of the 30- to 60-day oscillation and the genesis of tropical cyclones in the Western Pacific. *Max-Planck-Institut für Meteorologie Report* **64**

Wallace, J.M. and R.E. Dickinson, 1972: Empirical orthogonal representation of time series in the frequency domain. Part I: Theoretical considerations. *J. Appl. Meteor.* **11**, 887- 892

Weinberger, U., 1991: Die Reisekostenabrechnungen des Herrn Dr. von Storch. Hans-Albers-Verlag, Hamburg, 2714pp.

Xu, J., 1990: Analysis and prediction of the El Nino Southern Oscillation phenomenon using Principal Oscillation Pattern Analysis. *Max-Planck-Institut für Meteorologie Examensarbeiten* **4** (Max-Planck-Institut für Meteorologie; Bundesstrasse 55; 2000 Hamburg 13, Germany)

Xu, J., 1991a: On the relationship between the stratospheric QBO and the tropospheric SO. - *J. Atmos. Sci.*, in press

Xu, J., 1991b: The observed global low frequency variability in the atmosphere-ocean system from 1967 to 1986.- in preparation

Xu, J. and H. von Storch, 1990: "Principal Oscillation Patterns"-prediction of the state of ENSO. - *J. Climate* **3**, 1316-1329